Received: 27 October 2022 | Revised: 17 December 2023 | Accepted: 2 April 2024

DOI: 10.1002/acs.3810

RESEARCH ARTICLE

WILEY

Retrospective-cost-based model reference adaptive control of nonminimum-phase systems

Nima Mohseni | **Dennis S. Bernstein**

Department of Aerospace Engineering, University of Michigan, Ann Arbor, Michigan, USA

Correspondence
Nima Mohseni, Department of Aerospace Engineering, University of Michigan, 1320 Beal Ave., Ann Arbor, MI 48109, USA.
Email: nmohseni@umich.edu

Funding information
National Aeronautics and Space Administration, Grant/Award Number: 80NSSC20K1164

Abstract

This paper presents a novel approach to model reference adaptive control inspired by the adaptive pole-placement controller (APPC) of Elliot and based on retrospective cost optimization. Retrospective cost model reference adaptive control (RC-MRAC) is applicable to nonminimum-phase (NMP) systems assuming that the NMP zeros are known. Under this assumption, the advantage of RC-MRAC is a reduced need for persistency. The present paper compares APPC and RC-MRAC under various levels of persistency in the command for minimum-phase and NMP systems. It is shown numerically that the model-following performance of RC-MRAC is less sensitive to the persistency of the command compared to APPC at the cost of knowledge of the NMP zeros. RC-MRAC is also shown to be applicable for disturbance rejection under unknown harmonic disturbances.

KEYWORDS

adaptive control, disturbance rejection, model free control, model reference control, nonminimum-phase, pole placement

1 | INTRODUCTION

The objective of model reference adaptive control (MRAC) is to have the output of an uncertain system follow the response of a given reference system. The literature on MRAC and its applications is vast and varied, for example, References 1–3. MRAC methods can be divided into two categories, namely, indirect and direct. Indirect MRAC uses system identification followed by controller adaptation using the identified model, whereas direct MRAC adapts the controller using limited modeling information. Both types of methods typically use either gradient descent or recursive least squares for the adaptation.[4–7] MRAC methods have been extensively developed, including extensions to nonminimum-phase (NMP) and nonlinear systems.[8–14]

In the context of direct adaptive control, NMP systems are an important class of systems. These systems contain zeros outside of the unit disk and limit the achievable controller performance.[15] NMP systems also make development of direct adaptive control methods difficult since these methods tend to cancel unknown NMP zeros with a controller pole, leading to instability. Additionally, sampling a minimum-phase continuous-time system with relative degree greater than 2 leads to NMP discrete-time dynamics.[16]

A relevant method is the adaptive pole placement controller (APPC) developed in References 8,9,17, which can be applied to NMP systems with *unknown* NMP zeros. This is accomplished by overparameterizing the $2n$ parameter

controller identification problem as a $4n$ parameter problem using a Bezout identity. The drawback of this approach is the need for sufficient persistency in order to achieve model-following, even for step commands. Although this requirement was alleviated in Reference 18 through the use of dynamic regressor extension and mixing (DREM), the need for persistency is nontrivial.

The present paper develops a novel MRAC technique based on retrospective cost adaptive control (RCAC) and compares it with APPC. RCAC is a direct adaptive control method for command following and disturbance rejection for systems with uncertain dynamics and disturbance spectra.[19] For SISO discrete-time or sampled-data systems, RCAC requires knowledge of the sign of the leading numerator coefficient, relative degree, and NMP zeros. RCAC minimizes a retrospective performance measure based on the difference between filtered past control inputs and filtered, re-optimized past control inputs. To further reduce the dependence on prior modeling, an indirect adaptive control extension of RCAC was developed in Reference 20.

An early version of retrospective cost model reference adaptive control (RC-MRAC) was developed in Reference 21 with stability analysis given in Reference 22. A related technique was developed in Reference 23. Similarly to APPC, RC-MRAC uses recursive least squares for the adaptation law, which has a computational complexity of $O(n^2)$. As in the case of RCAC, RC-MRAC is applicable to discrete-time and sampled-data systems with known NMP zeros; minimum-phase zeros need not be known.

The goal and contribution of the present paper is to develop a new RC-MRAC method and assess its performance from the perspective of both command following and adaptive pole placement in comparison to APPC. Additionally, we show that, with minor modifications, RC-MRAC can perform disturbance rejection for harmonic disturbances with unknown spectra. The present paper significantly expands on the results in Reference 24. Numerical examples show that, in contrast to Reference 18, RC-MRAC does not require persistency. The price paid for alleviating the need for persistency is knowledge of the NMP zeros.

The structure of the paper is as follows, Section 2 gives an overview of the MRAC problem, Section 3 gives a derivation of APPC, Section 4 gives a derivation of RC-MRAC, Section 5 shows the connection between APPC and RC-MRAC, and Sections 6–8 provide examples and comparison of both algorithms for minimum- and NMP systems, as well as harmonic disturbance rejection.

2 | THE MODEL REFERENCE ADAPTIVE CONTROL PROBLEM

Consider the discrete-time SISO system

$$y_k = \frac{N(\mathbf{q}^{-1})}{D(\mathbf{q}^{-1})} u_k, \tag{1}$$

where

$$N(\mathbf{q}^{-1}) \triangleq \sum_{i=n_{\mathrm{r}}}^{n} N_i \mathbf{q}^{-i}, \tag{2}$$

$$D(\mathbf{q}^{-1}) \triangleq 1 + \sum_{i=1}^{n} D_i \mathbf{q}^{-i}, \tag{3}$$

are coprime, $N_{n_{\mathrm{r}}} \neq 0$, and n_{r} is the relative degree of $\frac{N(\mathbf{q}^{-1})}{D(\mathbf{q}^{-1})}$ as a rational function of $\mathbf{q}$. In the model reference adaptive control (MRAC) problem, the goal is to find a controller $G_{\mathrm{c}}(\mathbf{q}^{-1})$ such that the output y_k follows the desired reference response $y_{\mathrm{m},k}$ to a command r_k given by

$$y_{\mathrm{m},k} = \frac{N_{\mathrm{m}}(\mathbf{q}^{-1})}{D_{\mathrm{m}}(\mathbf{q}^{-1})} r_k, \tag{4}$$

where

$$N_{\mathrm{m}}(\mathbf{q}^{-1}) \triangleq \sum_{i=n_{\mathrm{r}}}^{n} N_{\mathrm{m},i} \mathbf{q}^{-i}, \tag{5}$$

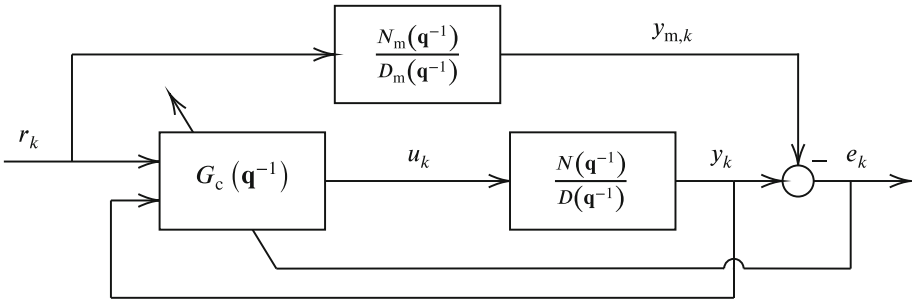

FIGURE 1 Block diagram of the direct model reference adaptive control problem.

$$D_{\mathrm{m}}(\mathbf{q}^{-1}) \triangleq 1 + \sum_{i=1}^{n} D_{\mathrm{m},i}\mathbf{q}^{-i}. \tag{6}$$

As shown in Figure 1, the error e_k between the actual plant response y_k and the reference model response $y_{\mathrm{m},k}$ is used to update the controller. The direct MRAC problem differs from the indirect case in that the plant is not identified, but knowledge of the NMP zeros of (1) is typically needed to prevent unstable pole-zero cancellation.

3 | ADAPTIVE POLE PLACEMENT CONTROLLER

The adaptive pole placement controller (APPC) developed in References 8,9 addresses the MRAC problem in the case where $N_{\mathrm{m}}(\mathbf{q}^{-1}) = N(\mathbf{q}^{-1})$. Through the use of a Bezout identity, no knowledge of the NMP zeros of the plant is needed and only the plant order n needs to be known. This comes at the cost of higher persistency of excitation requirements which has been previously demonstrated.[18] For reference, APPC is summarized below.

3.1 | APPC derivation

Defining

$$x_k \triangleq \frac{1}{D(\mathbf{q}^{-1})}u_k, \tag{7}$$

which satisfies

$$D(\mathbf{q}^{-1})x_k = u_k, \tag{8}$$

it follows that (1) can be written as

$$y_k = N(\mathbf{q}^{-1})x_k. \tag{9}$$

For the command r_k, consider the controller

$$u_k = N_{\mathrm{c}}(\mathbf{q}^{-1})y_k + D_{\mathrm{c}}(\mathbf{q}^{-1})u_k + H(\mathbf{q}^{-1})r_k, \tag{10}$$

where

$$N_{\mathrm{c}}(\mathbf{q}^{-1}) \triangleq \sum_{i=1}^{n} N_{\mathrm{c},i}\mathbf{q}^{-i}, \tag{11}$$

$$D_{\mathrm{c}}(\mathbf{q}^{-1}) \triangleq \sum_{i=1}^{n} D_{\mathrm{c},i}\mathbf{q}^{-i}, \tag{12}$$

$$H(\mathbf{q}^{-1}) \triangleq 1 + \sum_{i=1}^{n} H_i\mathbf{q}^{-i}, \tag{13}$$

and $H(\mathbf{q}^{-1})$ is an asymptotically stable monic polynomial as a function of $\mathbf{q}$. Combining (8), (9), and (10) yields

$$D(\mathbf{q}^{-1})x_k = N_{\mathrm{c}}(\mathbf{q}^{-1})N(\mathbf{q}^{-1})x_k + D_{\mathrm{c}}(\mathbf{q}^{-1})D(\mathbf{q}^{-1})x_k + H(\mathbf{q}^{-1})r_k, \tag{14}$$

which implies

$$x_k = \frac{H(\mathbf{q}^{-1})}{\tilde{D}(\mathbf{q}^{-1})}r_k, \tag{15}$$

where

$$\tilde{D}(\mathbf{q}^{-1}) \triangleq D(\mathbf{q}^{-1}) - N_{\mathrm{c}}(\mathbf{q}^{-1})N(\mathbf{q}^{-1}) - D_{\mathrm{c}}(\mathbf{q}^{-1})D(\mathbf{q}^{-1}). \tag{16}$$

Proposition 1. *Let the desired closed-loop poles be the roots of*

$$D_{\mathrm{m}}(\mathbf{q}^{-1}) = 1 + \sum_{i=1}^{n} D_{\mathrm{m},i}\mathbf{q}^{-i}, \tag{17}$$

and assume there exist $N_{\mathrm{c}}^*(\mathbf{q}^{-1})$ *and* $D_{\mathrm{c}}^*(\mathbf{q}^{-1})$ *such that*

$$D_{\mathrm{m}}(\mathbf{q}^{-1})H(\mathbf{q}^{-1}) = \tilde{D}^*(\mathbf{q}^{-1}), \tag{18}$$

where

$$\tilde{D}^*(\mathbf{q}^{-1}) \triangleq D(\mathbf{q}^{-1}) - N_{\mathrm{c}}^*(\mathbf{q}^{-1})N(\mathbf{q}^{-1}) - D_{\mathrm{c}}^*(\mathbf{q}^{-1})D(\mathbf{q}^{-1}). \tag{19}$$

Then, the closed-loop dynamics are given by

$$y_k = \frac{N(\mathbf{q}^{-1})}{D_{\mathrm{m}}(\mathbf{q}^{-1})}r_k. \tag{20}$$

Proof. Using (9), (15) with $\tilde{D}(\mathbf{q}^{-1}) = \tilde{D}^*(\mathbf{q}^{-1})$, and (18),

$$y_k = N(\mathbf{q}^{-1})x_k = \frac{N(\mathbf{q}^{-1})H(\mathbf{q}^{-1})}{\tilde{D}^*(\mathbf{q}^{-1})}r_k = \frac{N(\mathbf{q}^{-1})H(\mathbf{q}^{-1})}{D_{\mathrm{m}}(\mathbf{q}^{-1})H(\mathbf{q}^{-1})}r_k = \frac{N(\mathbf{q}^{-1})}{D_{\mathrm{m}}(\mathbf{q}^{-1})}r_k. \tag{21}$$

Note that, although the numerator of the closed loop dynamics (21) is $N(\mathbf{q}^{-1})$, Proposition 1 does not require knowledge of $N(\mathbf{q}^{-1})$. ∎

Proposition 2. *Let* $B^*(\mathbf{q}^{-1})$ *and* $C^*(\mathbf{q}^{-1})$ *satisfy the Bezout identity*

$$1 = B^*(\mathbf{q}^{-1})N(\mathbf{q}^{-1}) + C^*(\mathbf{q}^{-1})D(\mathbf{q}^{-1}), \tag{22}$$

where

$$B^*(\mathbf{q}^{-1}) \triangleq \sum_{i=1}^{n} B_i^*\mathbf{q}^{-i}, \tag{23}$$

$$C^*(\mathbf{q}^{-1}) \triangleq 1 + \sum_{i=1}^{n} C_i^*\mathbf{q}^{-i}. \tag{24}$$

Then,

$$\begin{aligned} &D_{\mathrm{m}}(\mathbf{q}^{-1})H(\mathbf{q}^{-1})[\tilde{B}(\mathbf{q}^{-1})y_k + \tilde{C}(\mathbf{q}^{-1})u_k] + [\tilde{N}_{\mathrm{c}}(\mathbf{q}^{-1})y_k + \tilde{D}_{\mathrm{c}}(\mathbf{q}^{-1})u_k] \\ &\quad = D_{\mathrm{m}}(\mathbf{q}^{-1})H(\mathbf{q}^{-1})[\hat{B}(\mathbf{q}^{-1})y_k + \hat{C}(\mathbf{q}^{-1})u_k] - [u_k - \hat{N}_{\mathrm{c}}(\mathbf{q}^{-1})y_k - \hat{D}_{\mathrm{c}}(\mathbf{q}^{-1})u_k], \end{aligned} \tag{25}$$

where

$$\tilde{B}(\mathbf{q}^{-1}) \triangleq \hat{B}(\mathbf{q}^{-1}) - B^*(\mathbf{q}^{-1}), \tag{26}$$

$$\tilde{C}(\mathbf{q}^{-1}) \triangleq \hat{C}(\mathbf{q}^{-1}) - C^*(\mathbf{q}^{-1}), \tag{27}$$

$$\tilde{N}_{\mathrm{c}}(\mathbf{q}^{-1}) \triangleq \hat{N}_{\mathrm{c}}(\mathbf{q}^{-1}) - N_{\mathrm{c}}^*(\mathbf{q}^{-1}), \tag{28}$$

$$\tilde{D}_{\mathrm{c}}(\mathbf{q}^{-1}) \triangleq \hat{D}_{\mathrm{c}}(\mathbf{q}^{-1}) - D_{\mathrm{c}}^*(\mathbf{q}^{-1}). \tag{29}$$

Proof. Multiplying both sides of (19) by x_k, and using (8), (9), and (18) yields

$$D_{\mathrm{m}}(\mathbf{q}^{-1})H(\mathbf{q}^{-1})x_k = u_k - N_{\mathrm{c}}^*(\mathbf{q}^{-1})y_k - D_{\mathrm{c}}^*(\mathbf{q}^{-1})u_k. \tag{30}$$

Multiplying both sides of (22) by x_k and using (8) and (9) yields

$$x_k = B^*(\mathbf{q}^{-1})y_k + C^*(\mathbf{q}^{-1})u_k. \tag{31}$$

Substituting (31) into (30) yields

$$D_{\mathrm{m}}(\mathbf{q}^{-1})H(\mathbf{q}^{-1})[B^*(\mathbf{q}^{-1})y_k + C^*(\mathbf{q}^{-1})u_k] = u_k - N_{\mathrm{c}}^*(\mathbf{q}^{-1})y_k - D_{\mathrm{c}}^*(\mathbf{q}^{-1})u_k. \tag{32}$$

Finally, substituting (26)–(29) into (32) yields (25). ∎

Note that all the terms on the right-hand side of (25) are known, and thus the sum of terms on the left-hand side is known despite the fact that $\tilde{N}_{\mathrm{c}}(\mathbf{q}^{-1})$, $\tilde{D}_{\mathrm{c}}(\mathbf{q}^{-1})$, $\tilde{B}(\mathbf{q}^{-1})$ and $\tilde{C}(\mathbf{q}^{-1})$ are individually unknown. Furthermore, if (26)–(29) are all zero, then both sides of (25) are zero. We thus define the performance variable

$$z_k \triangleq D_{\mathrm{m}}(\mathbf{q}^{-1})H(\mathbf{q}^{-1})[\hat{B}(\mathbf{q}^{-1})y_k + \hat{C}(\mathbf{q}^{-1})u_k] - [u_k - \hat{N}_{\mathrm{c}}(\mathbf{q}^{-1})y_k - \hat{D}_{\mathrm{c}}(\mathbf{q}^{-1})u_k] \tag{33}$$

$$= D_{\mathrm{m}}(\mathbf{q}^{-1})H(\mathbf{q}^{-1})[\tilde{B}(\mathbf{q}^{-1})y_k + \tilde{C}(\mathbf{q}^{-1})u_k] + [\tilde{N}_{\mathrm{c}}(\mathbf{q}^{-1})y_k + \tilde{D}_{\mathrm{c}}(\mathbf{q}^{-1})u_k]. \tag{34}$$

Note that, if $\tilde{N}_{\mathrm{c}}(\mathbf{q}^{-1})$, $\tilde{D}_{\mathrm{c}}(\mathbf{q}^{-1})$, $\tilde{B}(\mathbf{q}^{-1})$, and $\tilde{C}(\mathbf{q}^{-1})$ are all zero, then z_k is zero. We thus seek estimates $\hat{N}_{\mathrm{c}}(\mathbf{q}^{-1})$, $\hat{D}_{\mathrm{c}}(\mathbf{q}^{-1})$, $\hat{B}(\mathbf{q}^{-1})$ and $\hat{C}(\mathbf{q}^{-1})$ of $N_{\mathrm{c}}^*(\mathbf{q}^{-1})$, $D_{\mathrm{c}}^*(\mathbf{q}^{-1})$, $B^*(\mathbf{q}^{-1})$ and $C^*(\mathbf{q}^{-1})$, respectively, that minimize the magnitude of z_k.

3.2 | APPC algorithm

Proposition 3. *Define*

$$\theta_1 \triangleq \begin{bmatrix} N_{\mathrm{c},1}^* & \cdots & N_{\mathrm{c},n}^* & D_{\mathrm{c},1}^* & \cdots & D_{\mathrm{c},n}^* \end{bmatrix}^{\mathrm{T}}, \tag{35}$$

$$\theta_2 \triangleq \begin{bmatrix} B_{\mathrm{c},1}^* & \cdots & B_{\mathrm{c},n}^* & C_{\mathrm{c},1}^* & \cdots & C_{\mathrm{c},n}^* \end{bmatrix}^{\mathrm{T}}. \tag{36}$$

Then,

$$z_k = \begin{bmatrix} \Phi_k & \Phi_{\mathrm{f},k} \end{bmatrix} \begin{bmatrix} \theta_1 \\ \theta_2 \end{bmatrix} + u_{\mathrm{f},k}, \tag{37}$$

where

$$\Phi_k \triangleq \begin{bmatrix} y_{k-1} & \cdots & y_{k-n} & u_{k-1} & \cdots & u_{k-n} \end{bmatrix}, \tag{38}$$

$$\Phi_{\mathrm{f},k} \triangleq D_{\mathrm{m}}(\mathbf{q}^{-1})H(\mathbf{q}^{-1})\Phi_k, \tag{39}$$

$$u_{\mathrm{f},k} \triangleq [D_{\mathrm{m}}(\mathbf{q}^{-1})H(\mathbf{q}^{-1}) - 1]u_k. \tag{40}$$

Proof. Substituting (35), (36) and (38)–(40) into (33) yields (37). ∎

Since $N_{\mathrm{c}}^*(\mathbf{q}^{-1})$, $D_{\mathrm{c}}^*(\mathbf{q}^{-1})$, $B^*(\mathbf{q}^{-1})$ and $C^*(\mathbf{q}^{-1})$ are unknown, the goal is to solve the regression (37) at each step k to obtain estimates $\hat{\theta}_{1,k}$ and $\hat{\theta}_{2,k}$ of the polynomial coefficients θ_1 and θ_2, respectively. The estimation error is thus given by

$$\hat{z}_k(\hat{\theta}_{1,k}, \hat{\theta}_{2,k}) \triangleq \begin{bmatrix} \Phi_k & \Phi_{\mathrm{f},k} \end{bmatrix} \begin{bmatrix} \hat{\theta}_{1,k} \\ \hat{\theta}_{2,k} \end{bmatrix} + u_{\mathrm{f},k}. \tag{41}$$

For regression at each step, recursive least squares (RLS) is used to minimize the cost function

$$J_k(\hat{\theta}_{1,k}, \hat{\theta}_{2,k}) \triangleq \sum_{i=1}^{k} \lambda^{k-i}[\hat{z}_i(\hat{\theta}_{1,i}, \hat{\theta}_{2,i})^{\mathrm{T}}\hat{z}_i(\hat{\theta}_{1,i}, \hat{\theta}_{2,i})] + \lambda^k \left(\begin{bmatrix} \hat{\theta}_{1,k} \\ \hat{\theta}_{2,k} \end{bmatrix} - \begin{bmatrix} \hat{\theta}_{1,0} \\ \hat{\theta}_{2,0} \end{bmatrix} \right)^{\mathrm{T}} R_\theta \left(\begin{bmatrix} \hat{\theta}_{1,k} \\ \hat{\theta}_{2,k} \end{bmatrix} - \begin{bmatrix} \hat{\theta}_{1,0} \\ \hat{\theta}_{2,0} \end{bmatrix} \right), \tag{42}$$

where $\lambda \in (0, 1]$ is the forgetting factor. Using the computed RLS solution and (10), the control input at step $k+1$ is given by

$$u_{k+1} = \Phi_{k+1}\hat{\theta}_{1,k+1} + H(\mathbf{q}^{-1})r_{k+1}. \tag{43}$$

Note that the identified Bezout coefficients $\hat{B}(\mathbf{q}^{-1})$ and $\hat{C}(\mathbf{q}^{-1})$ are available from the RLS solution. However, these estimates are not used to determine the control input. In addition, $\hat{B}(\mathbf{q}^{-1})$ and $\hat{C}(\mathbf{q}^{-1})$ could be used to obtain estimates of $N(\mathbf{q}^{-1})$ and $D(\mathbf{q}^{-1})$. However, these estimates are not needed for APPC.

4 | RETROSPECTIVE COST MODEL REFERENCE ADAPTIVE CONTROL

4.1 | RC-MRAC derivation

Let $N(\mathbf{q}^{-1})$ be factored as

$$N(\mathbf{q}^{-1}) = N_{n_{\mathrm{r}}}N_{\mathrm{u}}(\mathbf{q}^{-1})N_{\mathrm{s}}(\mathbf{q}^{-1})\mathbf{q}^{-n_{\mathrm{r}}}, \tag{44}$$

where $N_{\mathrm{u}}(\mathbf{q}^{-1})$ and $N_{\mathrm{s}}(\mathbf{q}^{-1})$ as a function of $\mathbf{q}$ are monic polynomials of order n_{u} and n_{s} whose roots have modulus at least 1 and less than 1, respectively. Next, consider the controller

$$u_k = N_{\mathrm{c}}(\mathbf{q}^{-1})y_k + D_{\mathrm{c}}(\mathbf{q}^{-1})u_k + R_{\mathrm{c}}(\mathbf{q}^{-1})F(\mathbf{q}^{-1})r_k, \tag{45}$$

where $N_{\mathrm{c}}(\mathbf{q}^{-1})$ and $D_{\mathrm{c}}(\mathbf{q}^{-1})$ are given by (11) and (12), and

$$R_{\mathrm{c}}(\mathbf{q}^{-1}) \triangleq R_{\mathrm{c},0} + \sum_{i=1}^{n_{\mathrm{s}}} R_{\mathrm{c},i}\mathbf{q}^{-i}, \tag{46}$$

$$F(\mathbf{q}^{-1}) \triangleq 1 + \sum_{i=1}^{n-n_{\mathrm{s}}} F_i\mathbf{q}^{-i}, \tag{47}$$

where $F(\mathbf{q}^{-1})$ is an arbitrary stable monic polynomial in $\mathbf{q}$. Combining (8), (9), and (45) yields

$$D(\mathbf{q}^{-1})x_k = N_{\mathrm{c}}(\mathbf{q}^{-1})N(\mathbf{q}^{-1})x_k + D_{\mathrm{c}}(\mathbf{q}^{-1})D(\mathbf{q}^{-1})x_k + R_{\mathrm{c}}(\mathbf{q}^{-1})F(\mathbf{q}^{-1})r_k, \tag{48}$$

which implies

$$x_k = \frac{R_{\mathrm{c}}(\mathbf{q}^{-1})F(\mathbf{q}^{-1})}{\tilde{D}(\mathbf{q}^{-1})} r_k, \tag{49}$$

where

$$\tilde{D}(\mathbf{q}^{-1}) \triangleq D(\mathbf{q}^{-1}) - N_{\mathrm{c}}(\mathbf{q}^{-1})N(\mathbf{q}^{-1}) - D_{\mathrm{c}}(\mathbf{q}^{-1})D(\mathbf{q}^{-1}). \tag{50}$$

Proposition 4. *Let the desired closed-loop poles be the roots of*

$$D_{\mathrm{m}}(\mathbf{q}^{-1}) = 1 + \sum_{i=1}^{n} D_{\mathrm{m},i}\mathbf{q}^{-i}, \tag{51}$$

and assume there exist $N_{\mathrm{c}}^*(\mathbf{q}^{-1})$ *and* $D_{\mathrm{c}}^*(\mathbf{q}^{-1})$ *such that*

$$D_{\mathrm{m}}(\mathbf{q}^{-1})N_{\mathrm{s}}(\mathbf{q}^{-1})F(\mathbf{q}^{-1}) = \tilde{D}^*(\mathbf{q}^{-1}), \tag{52}$$

where

$$\tilde{D}^*(\mathbf{q}^{-1}) \triangleq D(\mathbf{q}^{-1}) - N_{\mathrm{c}}^*(\mathbf{q}^{-1})N(\mathbf{q}^{-1}) - D_{\mathrm{c}}^*(\mathbf{q}^{-1})D(\mathbf{q}^{-1}). \tag{53}$$

Then, the closed-loop dynamics are given by

$$y_k = \frac{N_{n_{\mathrm{r}}}N_u(\mathbf{q}^{-1})R_{\mathrm{c}}(\mathbf{q}^{-1})\mathbf{q}^{-n_{\mathrm{r}}}}{D_{\mathrm{m}}(\mathbf{q}^{-1})} r_k. \tag{54}$$

Proof. Using (9), (49) with $\tilde{D}(\mathbf{q}^{-1}) = \tilde{D}^*(\mathbf{q}^{-1})$, and (52),

$$y_k = N(\mathbf{q}^{-1})x_k = \frac{N(\mathbf{q}^{-1})R_{\mathrm{c}}(\mathbf{q}^{-1})F(\mathbf{q}^{-1})}{\tilde{D}^*(\mathbf{q}^{-1})} r_k = \frac{N(\mathbf{q}^{-1})R_{\mathrm{c}}(\mathbf{q}^{-1})F(\mathbf{q}^{-1})}{D_{\mathrm{m}}(\mathbf{q}^{-1})N_{\mathrm{s}}(\mathbf{q}^{-1})F(\mathbf{q}^{-1})} r_k = \frac{N_{n_{\mathrm{r}}}N_u(\mathbf{q}^{-1})R_{\mathrm{c}}(\mathbf{q}^{-1})\mathbf{q}^{-n_{\mathrm{r}}}}{D_{\mathrm{m}}(\mathbf{q}^{-1})} r_k.$$

■

Proposition 5. *Assume there exists* $R_{\mathrm{c}}^*(\mathbf{q}^{-1})$ *such that*

$$N_{\mathrm{m}}(\mathbf{q}^{-1}) = N_{n_{\mathrm{r}}}N_u(\mathbf{q}^{-1})R_{\mathrm{c}}^*(\mathbf{q}^{-1})\mathbf{q}^{-n_{\mathrm{r}}}, \tag{55}$$

and let

$$\tilde{N}_{\mathrm{c}}(\mathbf{q}^{-1}) \triangleq \hat{N}_{\mathrm{c}}(\mathbf{q}^{-1}) - N_{\mathrm{c}}^*(\mathbf{q}^{-1}), \tag{56}$$

$$\tilde{D}_{\mathrm{c}}(\mathbf{q}^{-1}) \triangleq \hat{D}_{\mathrm{c}}(\mathbf{q}^{-1}) - D_{\mathrm{c}}^*(\mathbf{q}^{-1}), \tag{57}$$

$$\tilde{R}_{\mathrm{c}}(\mathbf{q}^{-1}) \triangleq \hat{R}_{\mathrm{c}}(\mathbf{q}^{-1}) - R_{\mathrm{c}}^*(\mathbf{q}^{-1}). \tag{58}$$

Then,

$$\begin{aligned} &N_{n_{\mathrm{r}}}N_u(\mathbf{q}^{-1})\mathbf{q}^{-n_{\mathrm{r}}}[\tilde{N}_{\mathrm{c}}(\mathbf{q}^{-1})y_k + \tilde{D}_{\mathrm{c}}(\mathbf{q}^{-1})u_k + \tilde{R}_{\mathrm{c}}(\mathbf{q}^{-1})r_k] \\ &\quad = D_{\mathrm{m}}(\mathbf{q}^{-1})F(\mathbf{q}^{-1})(y_k - y_{\mathrm{m},k}) - N_{n_{\mathrm{r}}}N_u(\mathbf{q}^{-1})\mathbf{q}^{-n_{\mathrm{r}}}[u_k - \hat{N}_{\mathrm{c}}(\mathbf{q}^{-1})y_k - \hat{D}_{\mathrm{c}}(\mathbf{q}^{-1})u_k - \hat{R}_{\mathrm{c}}(\mathbf{q}^{-1})r_k] \end{aligned} \tag{59}$$

Proof. Multiplying both sides of (53) by x_k, and using (8), (9), and (52) yields

$$D_{\mathrm{m}}(\mathbf{q}^{-1})N_{\mathrm{s}}(\mathbf{q}^{-1})F(\mathbf{q}^{-1})x_k = u_k - N_{\mathrm{c}}^*(\mathbf{q}^{-1})y_k - D_{\mathrm{c}}^*(\mathbf{q}^{-1})u_k. \tag{60}$$

Then, multiplying both sides of (60) by $N_{n_r}N_u(\mathbf{q}^{-1})\mathbf{q}^{-n_r}$ and using (9) yields

$$D_m(\mathbf{q}^{-1})F(\mathbf{q}^{-1})y_k = N_{n_r}N_u(\mathbf{q}^{-1})\mathbf{q}^{-n_r}[u_k - N_c^*(\mathbf{q}^{-1})y_k - D_c^*(\mathbf{q}^{-1})u_k]. \tag{61}$$

Subtracting $F(\mathbf{q}^{-1})N_m(\mathbf{q}^{-1})r_k$ from both sides of (61) and using (4) yields

$$D_m(\mathbf{q}^{-1})F(\mathbf{q}^{-1})(y_k - y_{m,k}) = N_{n_r}N_u(\mathbf{q}^{-1})\mathbf{q}^{-n_r}[u_k - N_c^*(\mathbf{q}^{-1})y_k - D_c^*(\mathbf{q}^{-1})u_k] - F(\mathbf{q}^{-1})N_m(\mathbf{q}^{-1})r_k. \tag{62}$$

Then, combining (55) with (62) yields

$$D_m(\mathbf{q}^{-1})F(\mathbf{q}^{-1})(y_k - y_{m,k}) - N_{n_r}N_u(\mathbf{q}^{-1})\mathbf{q}^{-n_r}[u_k - N_c^*(\mathbf{q}^{-1})y_k - D_c^*(\mathbf{q}^{-1})u_k - R_c^*(\mathbf{q}^{-1})F(\mathbf{q}^{-1})r_k] = 0. \tag{63}$$

Substituting (56)–(58) into (63) yields (59). ∎

Note that all the terms on the right-hand side of (59) are known, and thus the sum of terms on the left-hand side is known despite the fact that $\tilde{N}_c(\mathbf{q}^{-1})$, $\tilde{D}_c(\mathbf{q}^{-1})$, and $\tilde{R}_c(\mathbf{q}^{-1})$ are individually unknown. Furthermore, if (56)–(58) are all zero, then both sides of (59) are zero. We thus define the performance variable

$$z_k \triangleq D_m(\mathbf{q}^{-1})F(\mathbf{q}^{-1})(y_k - y_{m,k}) - N_{n_r}N_u(\mathbf{q}^{-1})\mathbf{q}^{-n_r}[u_k - \hat{N}_c(\mathbf{q}^{-1})y_k - \hat{D}_c(\mathbf{q}^{-1})u_k - \hat{R}_c(\mathbf{q}^{-1})F(\mathbf{q}^{-1})r_k] \tag{64}$$

$$= N_{n_r}N_u(\mathbf{q}^{-1})\mathbf{q}^{-n_r}[\tilde{N}_c(\mathbf{q}^{-1})y_k + \tilde{D}_c(\mathbf{q}^{-1})u_k + \tilde{R}_c(\mathbf{q}^{-1})F(\mathbf{q}^{-1})r_k]. \tag{65}$$

Note that, if $\tilde{N}_c(\mathbf{q}^{-1})$, $\tilde{D}_c(\mathbf{q}^{-1})$, and $\tilde{R}_c(\mathbf{q}^{-1})$ are all zero, then z_k is zero. We thus seek estimates $\hat{N}_c(\mathbf{q}^{-1})$, $\hat{D}_c(\mathbf{q}^{-1})$, and $\hat{R}_c(\mathbf{q}^{-1})$ of $N_c^*(\mathbf{q}^{-1})$, $D_c^*(\mathbf{q}^{-1})$, and $R_c^*(\mathbf{q}^{-1})$, respectively, that minimize the magnitude of z_k.

4.2 | RC-MRAC algorithm

Proposition 6. *Define*

$$\theta \triangleq \begin{bmatrix} N_{c,1}^* & \cdots & N_{c,n}^* & D_{c,1}^* & \cdots & D_{c,n}^* & R_{c,0}^* & \cdots & R_{c,n_s}^* \end{bmatrix}^{\mathrm{T}}, \tag{66}$$

Then,

$$z_k = z_{f,k} - u_{f,k} + \Phi_{f,k}\theta, \tag{67}$$

where

$$r_{f,k} \triangleq F(\mathbf{q}^{-1})r_k \tag{68}$$

$$\Phi_k \triangleq \begin{bmatrix} y_{k-1} & \cdots & y_{k-n} & u_{k-1} & \cdots & u_{k-n} & r_{f,k} & \cdots & r_{f,k-n_s} \end{bmatrix}, \tag{69}$$

$$\Phi_{f,k} \triangleq N_{n_r}N_u(\mathbf{q}^{-1})\mathbf{q}^{-n_r}\Phi_k, \tag{70}$$

$$u_{f,k} \triangleq N_{n_r}N_u(\mathbf{q}^{-1})\mathbf{q}^{-n_r}u_k. \tag{71}$$

$$z_{f,k} \triangleq D_m(\mathbf{q}^{-1})F(\mathbf{q}^{-1})(y_k - y_{m,k}). \tag{72}$$

Proof. Substituting (66), and (68)–(72) into (64) yields (67). ∎

Since $N_c^*(\mathbf{q}^{-1})$, $D_c^*(\mathbf{q}^{-1})$, and $R_c^*(\mathbf{q}^{-1})$ are unknown, the goal is to solve the regression (67) at each step k to obtain the estimate $\hat{\theta}_k$. The estimation error is thus given by

$$\hat{z}_k(\hat{\theta}_k) \triangleq z_{f,k} - u_{f,k} + \Phi_{f,k}\hat{\theta}_k. \tag{73}$$

Algorithm 1. RC-MRAC

Initialize: $N_{n_r}, N_u(\mathbf{q}^{-1}), n_r, n_s, F(\mathbf{q}^{-1}), N_m(\mathbf{q}^{-1}), D_m(\mathbf{q}^{-1}), r_{f,0} = r_0, P_0 = R_\theta^{-1}$ positive-definite, $\lambda \in (0,1]$, $k = 0$, controller coefficients $\hat{\theta}_k$ initialized as 0, and the regressor Φ_k initialized as $\Phi_k = \begin{bmatrix} 0_{1\times 2n} & r_{f,0} & 0_{1\times n_s} \end{bmatrix}$

function RC-MRAC(y_k, u_k, r_k, r_{k+1})

Compute the reference model measurement

$y_{m,k} \leftarrow \frac{N_m(\mathbf{q}^{-1})}{D_m(\mathbf{q}^{-1})} r_k$

Filter command, regressor, control, and tracking error

$r_{f,k+1} \leftarrow F(\mathbf{q}^{-1}) r_{k+1}$

$\Phi_{f,k} \leftarrow N_{n_r} N_u(\mathbf{q}^{-1}) \mathbf{q}^{-n_r} \Phi_k$

$u_{f,k} \leftarrow N_{n_r} N_u(\mathbf{q}^{-1}) \mathbf{q}^{-n_r} u_k$

$z_{f,k} \leftarrow D_m(\mathbf{q}^{-1}) F(\mathbf{q}^{-1})(y_k - y_{m,k})$

Compute the performance variable

$z_k \leftarrow z_{f,k} - u_{f,k} + \Phi_{f,k} \hat{\theta}_k$

Update the controller coefficients using RLS

$P_{k+1} \leftarrow \frac{1}{\lambda} P_k - \frac{1}{\lambda} P_k \Phi_k^{\mathrm{T}} (\lambda + \Phi_k P_k \Phi_k^{\mathrm{T}})^{-1} \Phi_k P_k$

$\hat{\theta}_{k+1} \leftarrow \hat{\theta}_k + P_{k+1} \Phi_k^{\mathrm{T}} z_k$

$\Phi_{k+1} \leftarrow \Phi_k$

Update the regressor Φ_{k+1} with $y_k, u_k, r_{f,k+1}$, where $\Phi_k = \begin{bmatrix} y_{k-1} & \cdots & y_{k-n} & u_{k-1} & \cdots & u_{k-n} & r_{f,k} & \cdots & r_{f,k-n_s} \end{bmatrix}$

Compute control input

$u_{k+1} \leftarrow \Phi_{k+1} \hat{\theta}_{k+1}$

$k \leftarrow k + 1$

end function

For regression at each step, RLS is used to minimize the cost function

$$J_k(\hat{\theta}_k) \triangleq \sum_{i=1}^{k} \lambda^{k-i} [\hat{z}_i(\hat{\theta}_i)^{\mathrm{T}} \hat{z}_i(\hat{\theta}_i)] + \lambda^k (\hat{\theta}_k - \hat{\theta}_0)^{\mathrm{T}} R_\theta (\hat{\theta}_k - \hat{\theta}_0), \tag{74}$$

where $\lambda \in (0,1]$ is the forgetting factor. Using the computed RLS solution and (45), the control input at step $k+1$ is given by

$$u_{k+1} = \Phi_{k+1} \hat{\theta}_{k+1}. \tag{75}$$

Note that N_{n_r}, $N_u(\mathbf{q}^{-1})$, n_r, and n are assumed to be known a priori. A pseudocode implementation of the algorithm is given in Algorithm 1.

5 | CONNECTION BETWEEN RC-MRAC AND APPC

In the following section, we show that in the special case where $N_m(\mathbf{q}^{-1}) = N(\mathbf{q}^{-1})$, and $H(\mathbf{q}^{-1}) = N_s(\mathbf{q}^{-1}) F(\mathbf{q}^{-1})$, APPC and RC-MRAC are equivalent.

Proposition 7. *Let* $H(\mathbf{q}^{-1}) = N_s(\mathbf{q}^{-1}) F(\mathbf{q}^{-1})$, *and* $N_m(\mathbf{q}^{-1}) = N(\mathbf{q}^{-1})$ *such that* $R_c^*(\mathbf{q}^{-1}) = N_s(\mathbf{q}^{-1})$. *Then*, (63) *is equivalent to* (32).

Proof. Substituting $R_c^*(\mathbf{q}^{-1}) = N_s(\mathbf{q}^{-1})$ into (63) yields

$$D_m(\mathbf{q}^{-1}) F(\mathbf{q}^{-1})(y_k - y_{m,k}) - N_{n_r} N_u(\mathbf{q}^{-1}) \mathbf{q}^{-n_r} [u_k - N_c^*(\mathbf{q}^{-1}) y_k - D_c^*(\mathbf{q}^{-1}) u_k - N_s(\mathbf{q}^{-1}) F(\mathbf{q}^{-1}) r_k] = 0. \tag{76}$$

Using (4) and (55) in (76),

$$\begin{aligned} &D_{\mathrm{m}}(\mathbf{q}^{-1})F(\mathbf{q}^{-1})y_k - F(\mathbf{q}^{-1})N_{\mathrm{m}}(\mathbf{q}^{-1})r_k - N_{n_{\mathrm{r}}}N_u(\mathbf{q}^{-1})\mathbf{q}^{-n_{\mathrm{r}}}[u_k - N_{\mathrm{c}}^*(\mathbf{q}^{-1})y_k - D_{\mathrm{c}}^*(\mathbf{q}^{-1})u_k - N_{\mathrm{s}}(\mathbf{q}^{-1})F(\mathbf{q}^{-1})r_k] \\ &\quad = F(\mathbf{q}^{-1})D_{\mathrm{m}}(\mathbf{q}^{-1})y_k - F(\mathbf{q}^{-1})N_{\mathrm{m}}(\mathbf{q}^{-1})r_k - N_{n_{\mathrm{r}}}N_u(\mathbf{q}^{-1})\mathbf{q}^{-n_{\mathrm{r}}}[u_k - N_{\mathrm{c}}^*(\mathbf{q}^{-1})y_k - D_{\mathrm{c}}^*(\mathbf{q}^{-1})u_k] \\ &\qquad + N_{n_{\mathrm{r}}}N_u(\mathbf{q}^{-1})N_{\mathrm{s}}(\mathbf{q}^{-1})\mathbf{q}^{-n_{\mathrm{r}}}F(\mathbf{q}^{-1})r_k = 0. \end{aligned} \tag{77}$$

Using (55) in (77),

$$D_{\mathrm{m}}(\mathbf{q}^{-1})F(\mathbf{q}^{-1})y_k - N_{n_{\mathrm{r}}}N_u(\mathbf{q}^{-1})\mathbf{q}^{-n_{\mathrm{r}}}[u_k - N_{\mathrm{c}}^*(\mathbf{q}^{-1})y_k - D_{\mathrm{c}}^*(\mathbf{q}^{-1})u_k] = 0. \tag{78}$$

Then, substituting (9) into (78) and dividing by $N_{n_{\mathrm{r}}}N_u(\mathbf{q}^{-1})\mathbf{q}^{-n_{\mathrm{r}}}$ yields

$$\begin{aligned} &D_{\mathrm{m}}(\mathbf{q}^{-1})F(\mathbf{q}^{-1})N(\mathbf{q}^{-1})x_k - N_{n_{\mathrm{r}}}N_u(\mathbf{q}^{-1})\mathbf{q}^{-n_{\mathrm{r}}}[u_k - N_{\mathrm{c}}^*(\mathbf{q}^{-1})y_k - D_{\mathrm{c}}^*(\mathbf{q}^{-1})u_k] \\ &\quad = D_{\mathrm{m}}(\mathbf{q}^{-1})F(\mathbf{q}^{-1})N_{\mathrm{s}}(\mathbf{q}^{-1})x_k - [u_k - N_{\mathrm{c}}^*(\mathbf{q}^{-1})y_k - D_{\mathrm{c}}^*(\mathbf{q}^{-1})u_k] = 0. \end{aligned} \tag{79}$$

Substituting $N_{\mathrm{s}}(\mathbf{q}^{-1})F(\mathbf{q}^{-1}) = H(\mathbf{q}^{-1})$, and using the Bezout identity (31) yields the result

$$D_{\mathrm{m}}(\mathbf{q}^{-1})H(\mathbf{q}^{-1})[B^*(\mathbf{q}^{-1})y_k + C^*(\mathbf{q}^{-1})u_k] = u_k - N_{\mathrm{c}}^*(\mathbf{q}^{-1})y_k - D_{\mathrm{c}}^*(\mathbf{q}^{-1})u_k. \tag{80}$$

■

6 | EXAMPLE 1: STABLE MINIMUM-PHASE PLANT

Consider the plant

$$\frac{N(\mathbf{q}^{-1})}{D(\mathbf{q}^{-1})} = \frac{\mathbf{q}^{-1} - 0.5\mathbf{q}^{-2}}{(1 - \rho\exp(\jmath\nu)\mathbf{q}^{-1})(1 - \rho\exp(-\jmath\nu)\mathbf{q}^{-1})}, \tag{81}$$

and the desired model

$$\frac{N_{\mathrm{m}}(\mathbf{q}^{-1})}{D_{\mathrm{m}}(\mathbf{q}^{-1})} = \frac{\mathbf{q}^{-1} - 0.5\mathbf{q}^{-2}}{(1 - 0.5\exp(\jmath\frac{\pi}{2})\mathbf{q}^{-1})(1 - 0.5\exp(-\jmath\frac{\pi}{2})\mathbf{q}^{-1})}. \tag{82}$$

The following subsections demonstrate the model-following performance of APPC and RC-MRAC for various values of ρ and ν for step and harmonic commands. It is assumed that $N(\mathbf{q}^{-1})$ is known in order to compare the two algorithms. Each simulation is run for 200 steps, where the performance metric

$$\|e\| \triangleq \sqrt{\sum_{k=101}^{200} e_k^2}, \tag{83}$$

$$e_k \triangleq y_k - y_{\mathrm{m},k}, \tag{84}$$

is used to compare the algorithms.

6.1 | Example 1a: APPC for reference model following

For the APPC algorithm we choose

$$H(\mathbf{q}^{-1}) = N_{\mathrm{s}}(\mathbf{q}^{-1})F(\mathbf{q}^{-1}) = (1 - 0.5\mathbf{q}^{-1})(1 + 0.5\mathbf{q}^{-1}) = 1 - 0.25\mathbf{q}^{-2}, \tag{85}$$

and initialize $\hat{\theta}_{1,0} = 0_{4\times1}$ and $\hat{\theta}_{2,0} = 0_{4\times1}$ with $R_\theta = 10^{-5}I_8$ and $\lambda = 1$.

Given a unit step command for r_k, the model-following error versus the pole locations of the plant is shown in Figure 2A for various values of ρ and ν. Each point on the plot represents the location of the positive imaginary eigenvalue pole of the plant for its respective ρ and ν, and the color represents the model-following performance. Note that the

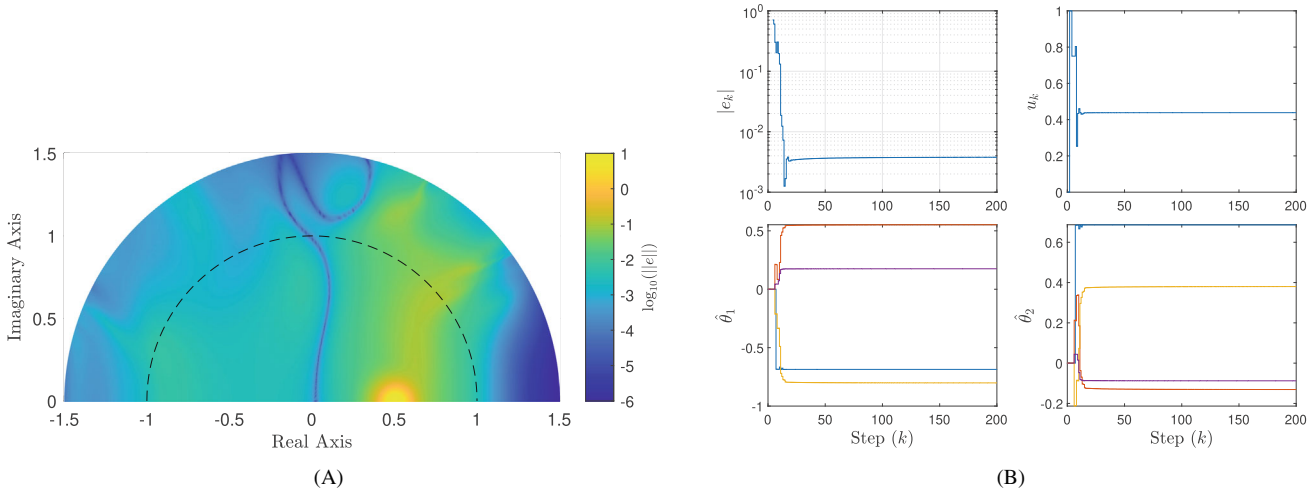

FIGURE 2 APPC for the minimum-phase plant (81) with a step command. (A) Log of the model-following error versus the pole locations of the plant. (B) Response of the system for $\rho = 0.5$ and $\nu = \frac{\pi}{4}$. Viewing clockwise from the top left: model-following error e_k, control input u_k, Bezout coefficient estimates $\hat{\theta}_2$, and controller coefficient estimates $\hat{\theta}_1$.

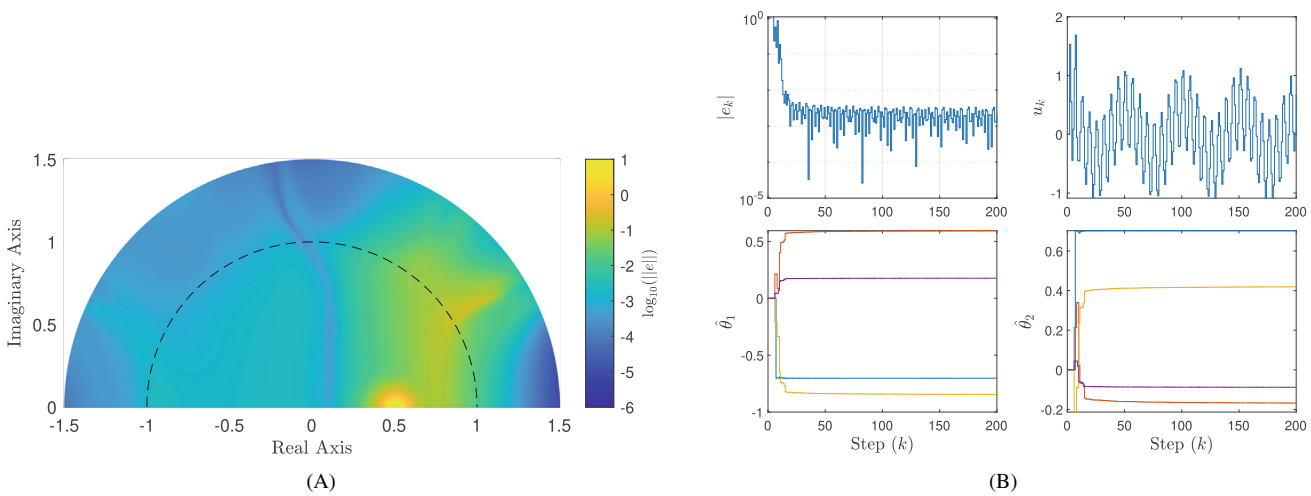

FIGURE 3 APPC for the minimum-phase plant (81) with a two-harmonic command. (A) Log of the model-following error versus the pole locations of the plant. (B) Response of the system for $\rho = 0.5$ and $\nu = \frac{\pi}{4}$. Viewing clockwise from the top left: model-following error e_k, control input u_k, Bezout coefficient estimates $\hat{\theta}_2$, and controller coefficient estimates $\hat{\theta}_1$.

model-following performance degrades as the plant poles move closer to the plant zero due to the system nearing a decrease in order. The response of the system for $\rho = 0.5$ and $\nu = \frac{\pi}{4}$ is given in Figure 2B.

Given the two-harmonic command $r_k = \cos(k) + \cos(\frac{1}{8}k)$, the model-following error versus the pole locations of the plant is shown in Figure 3A for various values of ρ and ν. Each point on the plot represents the location of the positive imaginary eigenvalue pole of the plant for its respective ρ and ν, and the color represents the model-following performance. Note that the model-following performance degrades as the plant poles move closer to the plant zero. The overall model-following error is improved compared to the step command. The response of the system for $\rho = 0.5$ and $\nu = \frac{\pi}{4}$ is given in Figure 3B.

Given the four-harmonic command $r_k = \cos(k) + \cos(\frac{1}{2}k) + \cos(\frac{1}{4}k) + \cos(\frac{1}{8}k)$, the model-following error versus the pole locations of the plant is shown in Figure 4A for various values of ρ and ν. Each point on the plot represents the location of the positive imaginary eigenvalue pole of the plant for its respective ρ and ν, and the color represents the model-following performance. Note that the model-following performance degrades as the plant poles move closer to the plant zero. Due to the increased persistency of the command, the model-following error is improved over both the step command and the two-harmonic command. The response of the system for $\rho = 0.5$ and $\nu = \frac{\pi}{4}$ is given in Figure 4B.

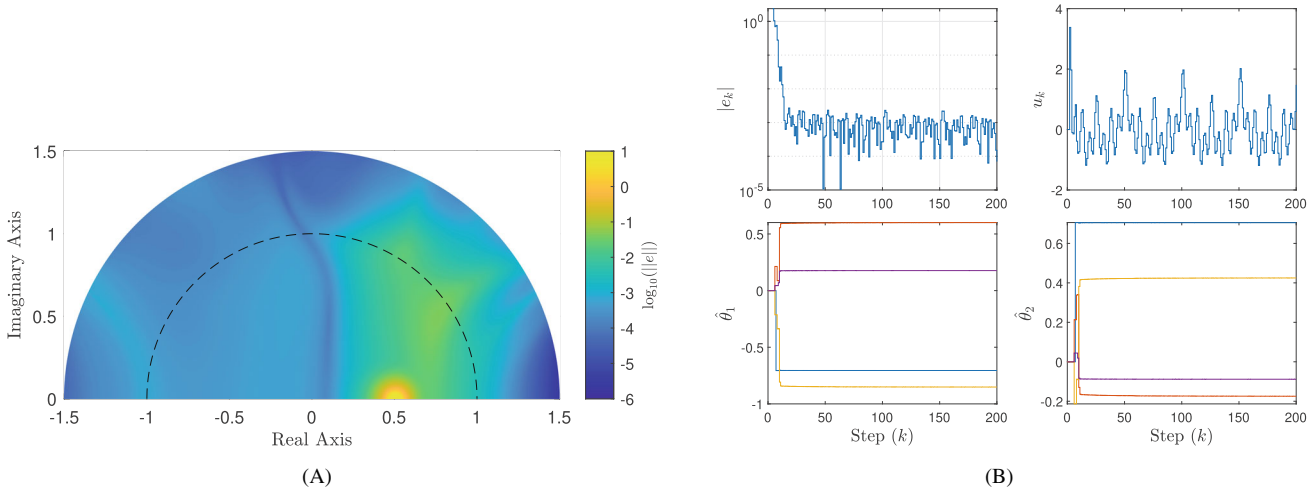

FIGURE 4 APPC for the minimum-phase plant (81) with a four-harmonic command. (A) Log of the model-following error versus the pole locations of the plant. (B) Response of the system for $\rho = 0.5$ and $\nu = \frac{\pi}{4}$. Viewing clockwise from the top left: model-following error e_k, control input u_k, Bezout coefficient estimates $\hat{\theta}_2$, and controller coefficient estimates $\hat{\theta}_1$.

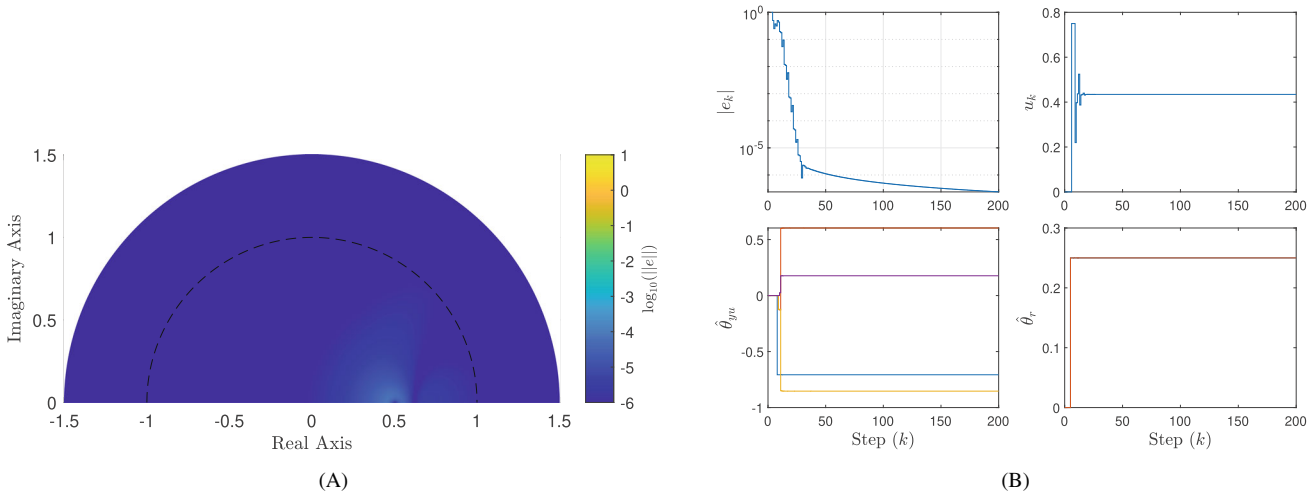

FIGURE 5 RC-MRAC for the minimum-phase plant (81) with a step command. (A) Log of the model-following error versus the pole locations of the plant. (B) Response of the system for $\rho = 0.5$ and $\nu = \frac{\pi}{4}$. Viewing clockwise from the top left: model-following error e_k, control input u_k, controller coefficients $\hat{\theta}$ associated with r_k, and controller coefficients $\hat{\theta}$ associated with y_k and u_k.

6.2 | Example 1b: RC-MRAC for reference model following

For RC-MRAC, we choose

$$F(\mathbf{q}^{-1}) = (1 + 0.5\mathbf{q}^{-1}), \tag{86}$$

and initialize $\hat{\theta}_0 = 0_{6\times1}$, with $R_\theta = 10^{-5}I_6$ and $\lambda = 1$.

Given a unit step command for r_k, the model-following error versus the pole locations of the plant is shown in Figure 5A for various values of ρ and ν. Each point on the plot represents the location of the positive imaginary eigenvalue pole of the plant for its respective ρ and ν, and the color represents the model-following performance. Note that the model-following performance degrades as the plant poles move closer to the plant zero. The response of the system for $\rho = 0.5$ and $\nu = \frac{\pi}{4}$ is given in Figure 5B.

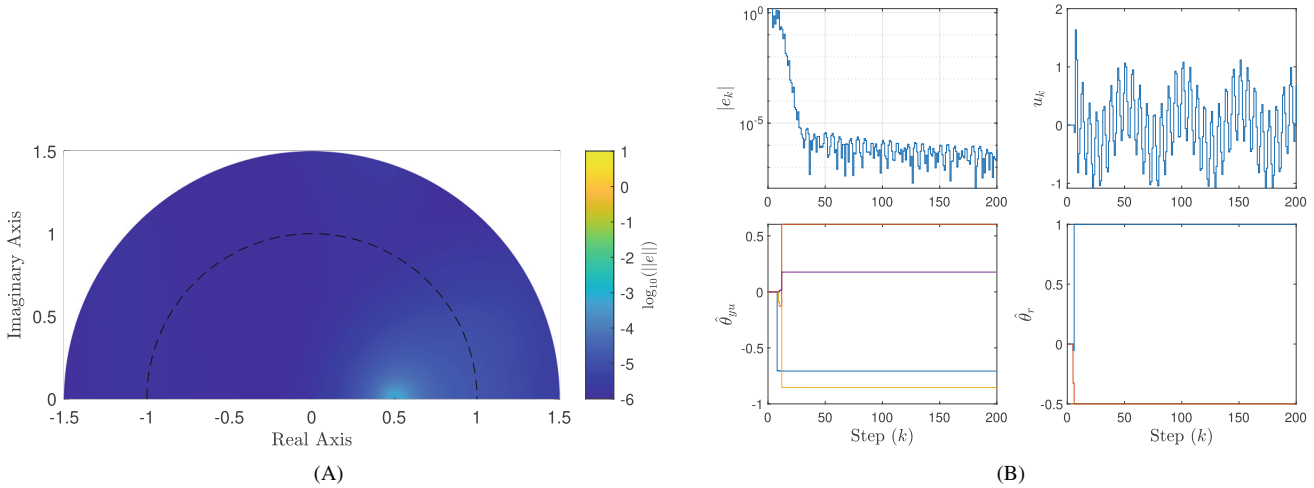

FIGURE 6 RC-MRAC for the minimum-phase plant (81) with a two-harmonic command. (A) Log of the model-following error versus the pole locations of the plant. (B) Response of the system for $\rho = 0.5$ and $\nu = \frac{\pi}{4}$. Viewing clockwise from the top left: model-following error e_k, control input u_k, controller coefficients $\hat{\theta}$ associated with r_k, and controller coefficients $\hat{\theta}$ associated with y_k and u_k.

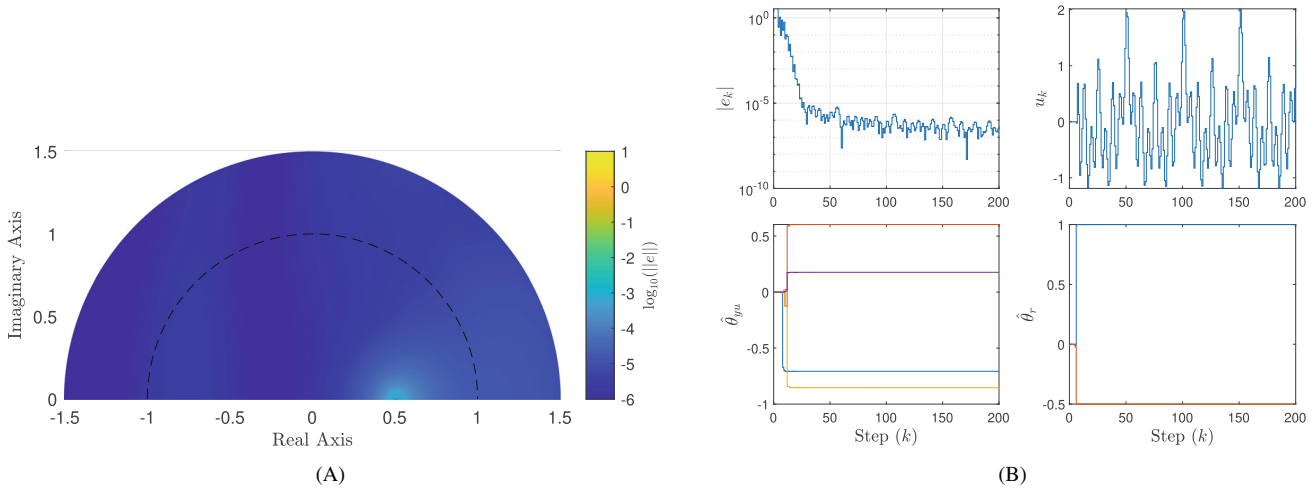

FIGURE 7 RC-MRAC for the minimum-phase plant (81) with a four-harmonic command. (A) Log of the model-following error versus the pole locations of the plant. (B) Response of the system for $\rho = 0.5$ and $\nu = \frac{\pi}{4}$. Viewing clockwise from the top left: model-following error e_k, control input u_k, controller coefficients $\hat{\theta}$ associated with r_k, and controller coefficients $\hat{\theta}$ associated with y_k and u_k.

Given the two-harmonic command $r_k = \cos(k) + \cos\left(\frac{1}{8}k\right)$, the model-following error versus the pole locations of the plant is shown in Figure 6A for various values of ρ and ν. Each point on the plot represents the location of the positive imaginary eigenvalue pole of the plant for its respective ρ and ν, and the color represents the model-following performance. Note that the model-following performance degrades as the plant poles move closer to the plant zero. The overall model-following error is similar to the step command. The response of the system for $\rho = 0.5$ and $\nu = \frac{\pi}{4}$ is given in Figure 6B.

Given the four-harmonic command $r_k = \cos(k) + \cos\left(\frac{1}{2}k\right) + \cos\left(\frac{1}{4}k\right) + \cos\left(\frac{1}{8}k\right)$, the model-following error versus the pole locations of the plant is shown in Figure 7A for various values of ρ and ν. Each point on the plot represents the location of the positive imaginary eigenvalue pole of the plant for its respective ρ and ν, and the color represents the model-following performance. Note that the model-following performance degrades as the plant poles move closer to the plant zero. The response of the system for $\rho = 0.5$ and $\nu = \frac{\pi}{4}$ is given in Figure 7B.

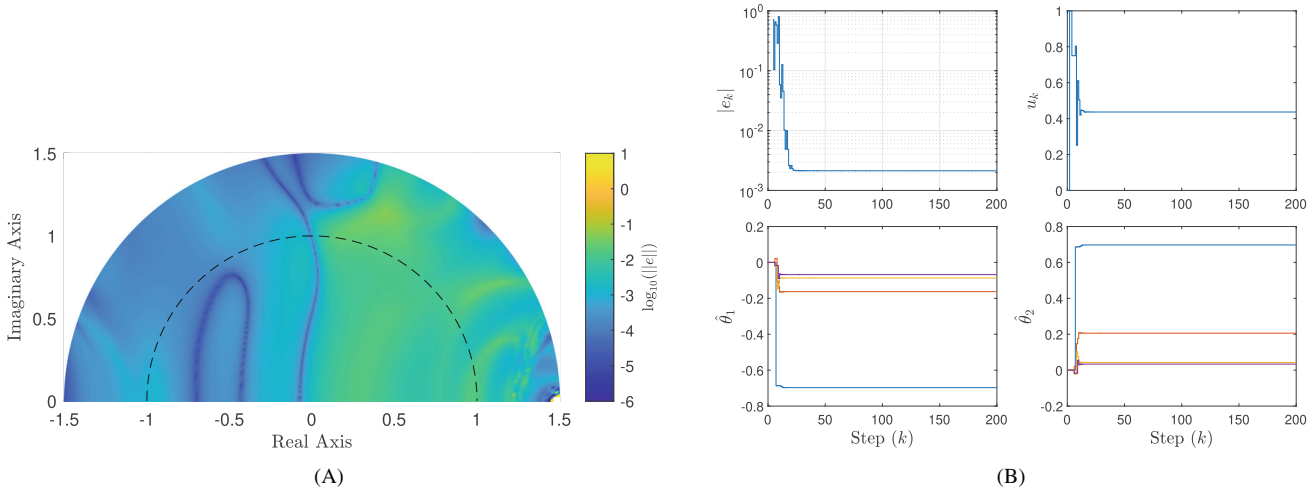

(A) (B)

FIGURE 8 APPC for the NMP plant (87) with a step command. (A) Log of the model-following error versus the pole locations of the plant. Empty squares represent regions where the system became unstable. (B) Response of the system for $\rho = 0.5$ and $\nu = \frac{\pi}{4}$. Viewing clockwise from the top left: model-following error e_k, control input u_k, Bezout coefficient estimates $\hat{\theta}_2$, and controller coefficient estimates $\hat{\theta}_1$.

7 | EXAMPLE 2: NONMINIMUM-PHASE PLANT

Consider the plant

$$\frac{N(\mathbf{q}^{-1})}{D(\mathbf{q}^{-1})} = \frac{\mathbf{q}^{-1} - 1.5\mathbf{q}^{-2}}{(1 - \rho\exp(\jmath\nu)\mathbf{q}^{-1})(1 - \rho\exp((-\jmath\nu)\mathbf{q}^{-1})}, \tag{87}$$

and the desired model

$$\frac{N_{\mathrm{m}}(\mathbf{q}^{-1})}{D_{\mathrm{m}}(\mathbf{q}^{-1})} = \frac{\mathbf{q}^{-1} - 1.5\mathbf{q}^{-2}}{(1 - 0.5\exp(\jmath\frac{\pi}{2})\mathbf{q}^{-1})(1 - 0.5\exp(-\jmath\frac{\pi}{2})\mathbf{q}^{-1})}. \tag{88}$$

The following subsections demonstrate the model-following performance of RC-MRAC and APPC for various values of ρ and ν for step and harmonic commands. It is assumed that $N(\mathbf{q}^{-1})$ is known in order to compare the two algorithms. The same performance metric (83) as in Example 1 is used.

7.1 | Example 2a: APPC for reference model following

For the APPC algorithm we choose

$$H(\mathbf{q}^{-1}) = 1 - 0.25\mathbf{q}^{-2}, \tag{89}$$

and initialize $\hat{\theta}_{1,0} = 0_{4\times1}$ and $\hat{\theta}_{2,0} = 0_{4\times1}$ with $R_\theta = 10^{-5}I_8$ and $\lambda = 1$.

Given a unit step command for r_k, the model-following error versus the pole locations of the plant is shown in Figure 8A for various values of ρ and ν. Each point on the plot represents the location of the positive imaginary eigenvalue pole of the plant for its respective ρ and ν, and the color represents the model-following performance. Note that the model-following performance degrades as the plant poles move closer to the plant zero. The response of the system for $\rho = 0.5$ and $\nu = \frac{\pi}{4}$ is given in Figure 8B.

Given the two-harmonic command $r_k = \cos(k) + \cos\left(\frac{1}{8}k\right)$, the model-following error versus the pole locations of the plant is shown in Figure 9A for various values of ρ and ν. Each point on the plot represents the location of the positive imaginary eigenvalue pole of the plant for its respective ρ and ν, and the color represents the model-following

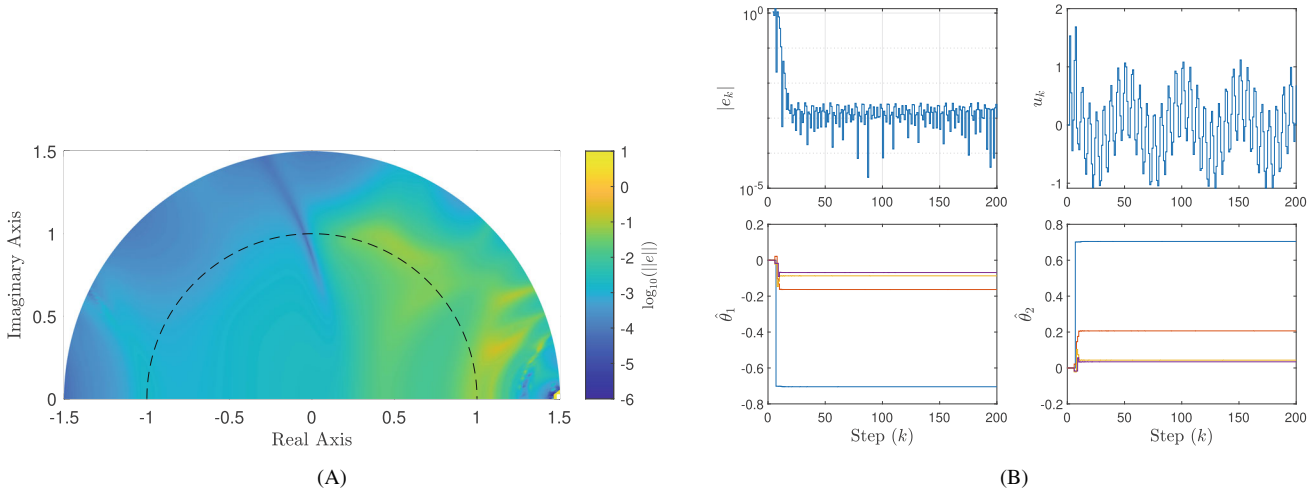

FIGURE 9 APPC for the NMP plant (87) with a two-harmonic command. (A) Log of the model-following error versus the pole locations of the plant. Empty squares represent regions where the system became unstable. (B) Response of the system for $\rho = 0.5$ and $\nu = \frac{\pi}{4}$. Viewing clockwise from the top left: model-following error e_k, control input u_k, Bezout coefficient estimates $\hat{\theta}_2$, and controller coefficient estimates $\hat{\theta}_1$.

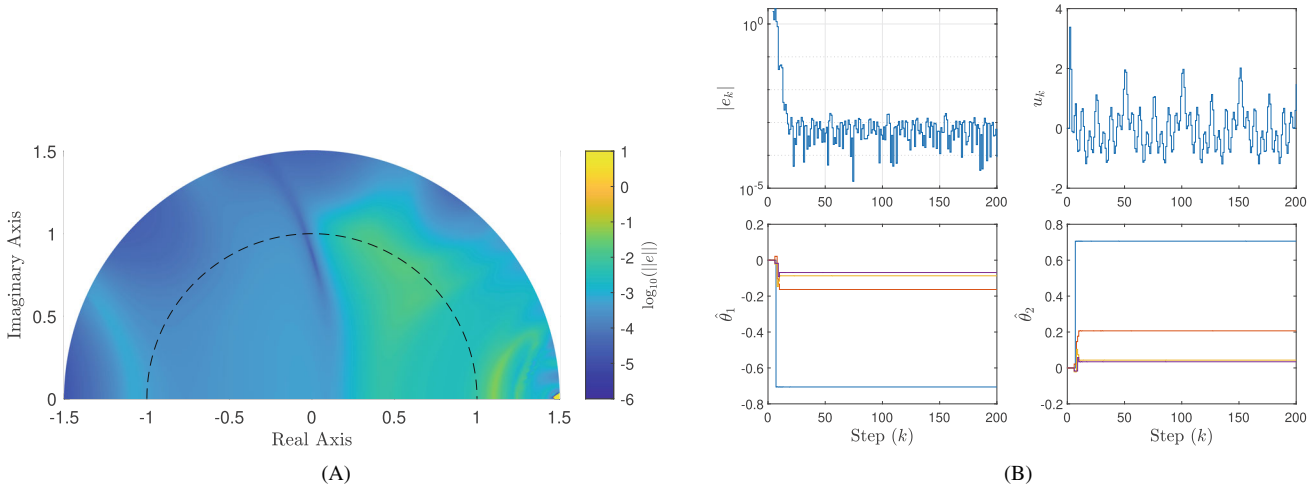

FIGURE 10 APPC for the NMP plant (87) with a four-harmonic command. (A) Log of the model-following error versus the pole locations of the plant. Empty squares represent regions where the system became unstable. (B) Response of the system for $\rho = 0.5$ and $\nu = \frac{\pi}{4}$. Viewing clockwise from the top left: model-following error e_k, control input u_k, Bezout coefficient estimates $\hat{\theta}_2$, and controller coefficient estimates $\hat{\theta}_1$.

performance. Note that the model-following performance degrades as the plant poles move closer to the plant zero. The overall model-following error is improved compared to the step command. The response of the system for $\rho = 0.5$ and $\nu = \frac{\pi}{4}$ is given in Figure 9B.

Given the four-harmonic command $r_k = \cos(k) + \cos\left(\frac{1}{2}k\right) + \cos\left(\frac{1}{4}k\right) + \cos\left(\frac{1}{8}k\right)$, the model-following error versus the pole locations of the plant is shown in Figure 10A for various values of ρ and ν. Each point on the plot represents the location of the positive imaginary eigenvalue pole of the plant for its respective ρ and ν, and the color represents the model-following performance. Note that the model-following performance degrades as the plant poles move closer to the plant zero. Due to the increased persistency of the command, the model-following error is improved over both the step command and the two-harmonic command. The response of the system for $\rho = 0.5$ and $\nu = \frac{\pi}{4}$ is given in Figure 10B.

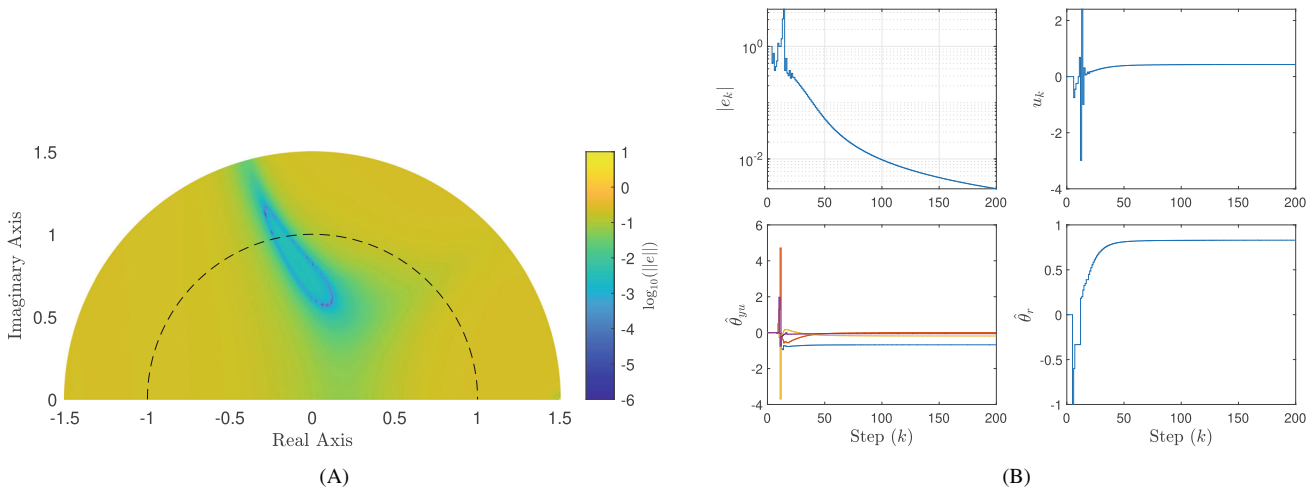

FIGURE 11 RC-MRAC for the NMP plant (87) with step command. (A) Log of the model-following error versus the pole locations of the plant. (B) Response of the system for $\rho = 0.5$ and $\nu = \frac{\pi}{4}$. Viewing clockwise from the top left: model-following error e_k, control input u_k, controller coefficients $\hat{\theta}$ associated with r_k, and controller coefficients $\hat{\theta}$ associated with y_k and u_k.

7.2 | Example 2b: RC-MRAC for reference model following

For RC-MRAC, we choose

$$F(\mathbf{q}^{-1}) = 1 - 0.25\mathbf{q}^{-2}, \tag{90}$$

and initialize $\hat{\theta}_0 = 0_{5\times1}$, with $R_\theta = 10^{-5}I_5$ and $\lambda = 1$. Given a unit step command for r_k, the model-following error versus the pole locations of the plant is shown in Figure 11A for various values of ρ and ν. Each point on the plot represents the location of the positive imaginary eigenvalue pole of the plant for its respective ρ and ν, and the color represents the model-following performance. Note that the model-following performance degrades as the plant poles move closer to the plant zero and that the convergence is much slower than in the minimum-phase case. The response of the system for $\rho = 0.5$ and $\nu = \frac{\pi}{4}$ is given in Figure 11B.

Given the two-harmonic command $r_k = \cos(k) + \cos\left(\frac{1}{8}k\right)$, the model-following error versus the pole locations of the plant is shown in Figure 12A for various values of ρ and ν. Each point on the plot represents the location of the positive imaginary eigenvalue pole of the plant for its respective ρ and ν, and the color represents the model-following performance. Note that the model-following performance degrades as the plant poles move closer to the plant zero. The overall model-following error is improved compared to the step command, but the controller convergence is still slower than the minimum-phase case. The response of the system for $\rho = 0.5$ and $\nu = \frac{\pi}{4}$ is given in Figure 12B.

Given the four-harmonic command $r_k = \cos(k) + \cos\left(\frac{1}{2}k\right) + \cos\left(\frac{1}{4}k\right) + \cos\left(\frac{1}{8}k\right)$, the model-following error versus the pole locations of the plant is shown in Figure 13A for various values of ρ and ν. Each point on the plot represents the location of the positive imaginary eigenvalue pole of the plant for its respective ρ and ν, and the color represents the model-following performance. Note that the model-following performance degrades as the plant poles move closer to the plant zero. Due to the increased persistency of the command, the model-following error is improved over both the step command and the two-harmonic command. The convergence of the controller is much slower than in the minimum-phase case. The response of the system for $\rho = 0.5$ and $\nu = \frac{\pi}{4}$ is given in Figure 13B.

8 | EXAMPLE 3: UNKNOWN HARMONIC DISTURBANCE REJECTION USING RC-MRAC

Consider the same system (81), and reference model (82), as in Example 1. We now place an unknown single harmonic disturbance at the frequency 0.35 radians per step at the input of the system. In this section we show that, unlike APPC,

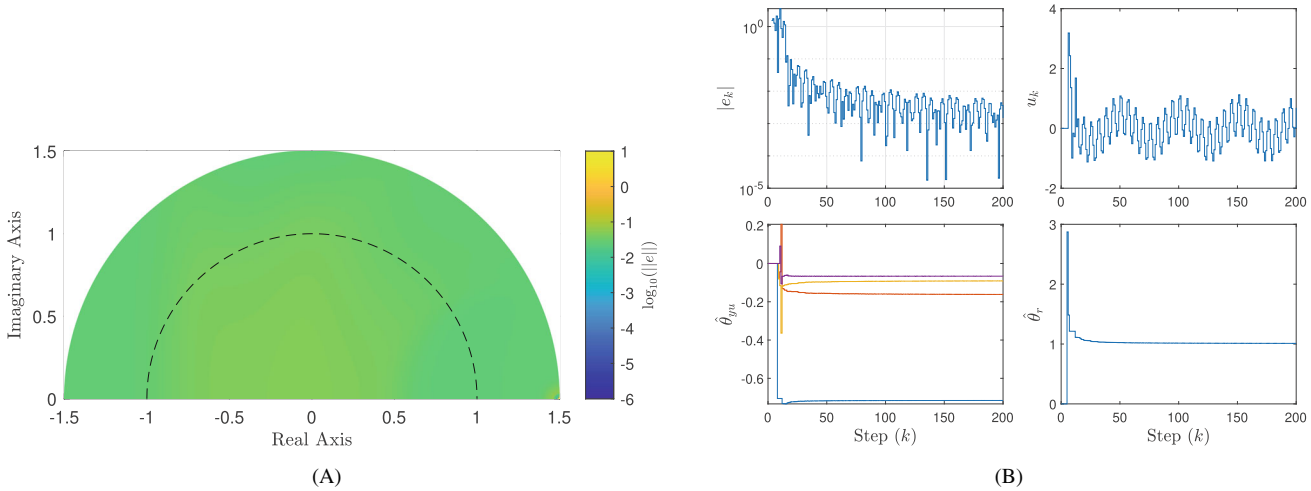

FIGURE 12 RC-MRAC for the NMP plant (87) with a two-harmonic command. (A) Log of the model-following error versus the pole locations of the plant. (B) Response of the system for $\rho = 0.5$ and $\nu = \frac{\pi}{4}$. Viewing clockwise from the top left: model-following error e_k, control input u_k, controller coefficients $\hat{\theta}$ associated with r_k, and controller coefficients $\hat{\theta}$ associated with y_k and u_k.

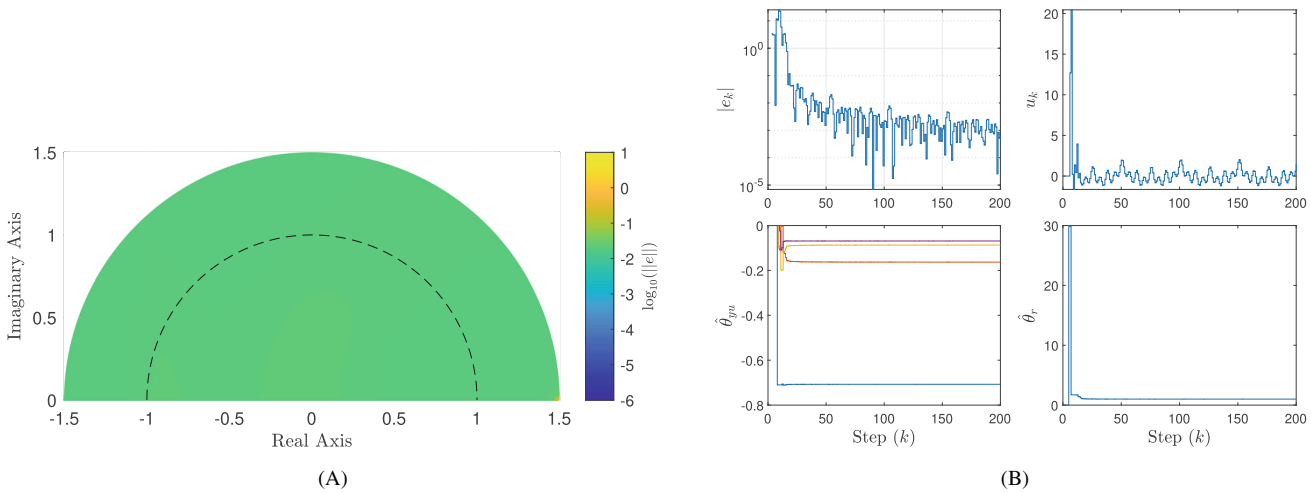

FIGURE 13 RC-MRAC for the NMP plant (87) with a four-harmonic command. (A) Log of the model-following error versus the pole locations of the plant. (B) Response of the system for $\rho = 0.5$ and $\nu = \frac{\pi}{4}$. Viewing clockwise from the top left: model-following error e_k, control input u_k, controller coefficients $\hat{\theta}$ associated with r_k, and controller coefficients $\hat{\theta}$ associated with y_k and u_k.

RC-MRAC can be used for disturbance rejection of unknown harmonic disturbances with a small modification. The disturbance rejection capability is tested for various values of ρ and ν for a step command on the reference model. It is assumed that $N(\mathbf{q}^{-1})$ is known. The same performance metric (83) as in Example 1 is used.

To accomplish harmonic disturbance rejection and model-following, we increase the order of the controller to $n = 4$, and set $n_s = 3$ to match the desired closed-loop model relative degree. The order must be incremented by 2 for each expected harmonic disturbance. The order can be larger than required at the cost of perfect model tracking. RLS is initialized with $\hat{\theta}_0 = 0_{12\times 1}$, $R_\theta = 10^{-5} I_{12}$ and $\lambda = 1$. $F(\mathbf{q}^{-1})$ is chosen to be (86), the same as in Example 1b.

Given a unit step command for r_k, the model-following error versus the pole locations of the plant is shown in Figure 14A for various values of ρ and ν. Each point on the plot represents the location of the positive imaginary eigenvalue pole of the plant for its respective ρ and ν, and the color represents the model-following performance. Note that the model-following performance degrades as the plant poles move closer to the plant zero, but the algorithm is able to perform the model-following task while rejecting the disturbance for all tested poles. The response of the system for $\rho = 0.5$ and $\nu = \frac{\pi}{4}$ is given in Figure 14B.

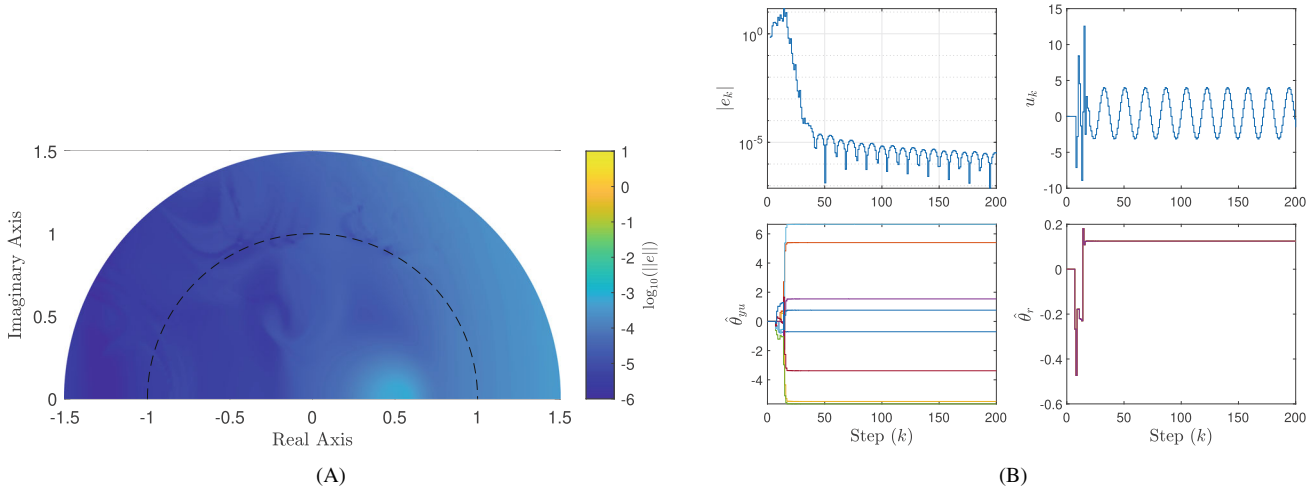

FIGURE 14 RC-MRAC for harmonic disturbance rejection on the plant (81) with a step command. (A) Log of the model-following error versus the pole locations of the plant. (B) Response of the system for $\rho = 0.5$ and $\nu = \frac{\pi}{4}$. Viewing clockwise from the top left: model-following error e_k, control input u_k, controller coefficients $\hat{\theta}$ associated with r_k, and controller coefficients $\hat{\theta}$ associated with y_k and u_k.

9 | SUMMARY OF EXAMPLES

In Sections 6 and 7, we demonstrate the reference model following performance of APPC and RC-MRAC under step commands and harmonic commands for various minimum- and nonminimum-phase systems. For minimum-phase systems, it is shown that as the persistency of the command increased, RC-MRAC is able to more closely follow the desired reference trajectory and performs similarly regardless of the persistency of the command whereas the performance of APPC depended on the persistency of the command. For NMP systems, RC-MRAC converges to a smaller model following error than APPC at lower persistency levels but has slower convergence times. Additionally, RC-MRAC's performance is consistent over the tested plant poles while APPC's performance is heavily dependent on the plant. For systems with harmonic disturbances, RC-MRAC is modified to treat the disturbance as a part of the plant, allowing for reference model following and disturbance rejection.

10 | CONCLUSIONS AND FUTURE RESEARCH

Retrospective cost model reference adaptive control (RC-MRAC) was developed and compared to Elliot's adaptive pole placement controller (APPC). This controller places the closed-loop poles of the system to match the desired closed-loop poles given by a reference model provided that the leading numerator coefficient, relative degree, system order, and NMP zeros are known. RC-MRAC was shown numerically to be stable over a wide range of systems. Unlike APPC, the performance of RC-MRAC is not as sensitive to the persistency of the desired command. Additionally, it was shown that, with a slight modification, RC-MRAC can reject harmonic disturbances. For minimum-phase systems, RC-MRAC outperforms APPC without the need for persistency. For NMP systems, RC-MRAC performs better than APPC at lower persistency levels at the price of knowledge of the NMP zeros and slower convergence times.

Future work will extend RC-MRAC to the MIMO case following a similar development for RCAC given in Reference 19. A key challenge is the development of stability results for RC-MRAC. Given the development of stability results for similar algorithms,[7,8] a stability result for RC-MRAC will closely follow established arguments.

ACKNOWLEDGMENTS

This work was supported by a NASA Space Technology Graduate Research Opportunity [grant number 80NSSC20K1164]. We appreciate numerous helpful suggestions provided by the reviewers.

ORCID

Nima Mohseni https://orcid.org/0000-0002-2031-3763

Dennis S. Bernstein https://orcid.org/0000-0003-0399-3039

REFERENCES

1. Leman T, Xargay E, Dullerud G, Hovakimyan N, Wendel T. L1 adaptive control augmentation system for the X-48B aircraft. *Proc AIAA Guid Nav Contr Conf*. 2012:1-14. doi:10.2514/6.2009-5619
2. Dydek ZT, Annaswamy AM, Lavretsky E. Adaptive control of quadrotor UAVs: a design trade study with flight evaluations. *IEEE Trans Contr Syst Tech*. 2013;21(4):1400-1406. doi:10.1109/TCST.2012.2200104
3. Chowdhary G, Kingravi HA, How JP, Vela PA. Bayesian nonparametric adaptive control using Gaussian processes. *IEEE Trans Neural Netw Learn Syst*. 2015;26(3):537-550. doi:10.1109/TNNLS.2014.2319052
4. Ioannou PA, Sun J. *Robust Adaptive Control*. Prentice-Hall; 1996.
5. Goodwin GC, Sin KS. *Adaptive Filtering, Prediction, and Control*. Prentice Hall; 1984.
6. ÅstrÖm KJ, Wittenmark B. *Adaptive Control*. 2nd ed. Addison-Wesley Longman Publishing Co., Inc; 1994.
7. Goodwin G, Ramadge P, Caines P. Discrete-time multivariable adaptive control. *IEEE Trans Autom Contr*. 1980;25(3):449-456. doi:10.1109/TAC.1980.1102363
8. Elliott H, Cristi R, Das M. Global stability of adaptive pole placement algorithms. *IEEE Trans Automat Contr*. 1985;30(4):348-356. doi:10.1109/TAC.1985.1103954
9. Elliott H. Direct adaptive pole placement with application to nonminimum phase systems. *IEEE Trans Automat Contr*. 1982;27(3):720-722. doi:10.1109/TAC.1982.1102963
10. Bayard D. Stable direct adaptive periodic control using only plant order knowledge. *Am Control Conf*. 1995;15:1092-1096. doi:10.1109/ACC.1995.520914
11. M'Saad M, Ortega R, Landau I. Adaptive controllers for discrete-time systems with arbitrary zeros: an overview. *Automatica*. 1985;21(4):413-423. doi:10.1016/0005-1098(85)90077-9
12. Kaufman H, Barkana I, Sobel K. *Direct Adaptive Control Algorithms: Theory and Applications*. Springer; 1998.
13. Åström KJ. Direct methods for nonminimum phase systems. IEEE Conference on Decision and Control Including the Symposium on Adaptive Processes, 611-615. 1980. doi:10.1109/CDC.1980.271868
14. Dai S, Ren Z, Bernstein DS. Adaptive control of nonminimum-phase systems using shifted Laurent series. *Int J Contr*. 2017;90:409-422.
15. Hoagg JB, Bernstein DS. Nonminimum-phase zeros: much to do about nothing. *IEEE Contr. Syst. Mag.* 2007;27:45-57.
16. Åström KJ, Hagander P, Sternby J. Zeros of sampled systems. *Automatica*. 1984;20(1):31-38. doi:10.1016/0005-1098(84)90062-1
17. Janecki D. Stability analysis of Elliott's direct adaptive pole placement. *Syst Control Lett*. 1988;11(1):19-26. doi:10.1016/0167-6911(88)90106-5
18. Pyrkin A, Ortega R, Gromov V, Bobtsov A, Vedyakov A. A globally convergent direct adaptive pole-placement controller for nonminimum phase systems with relaxed excitation assumptions. *Int J Adapt Control Signal Process*. 2019;33(10):1491-1505. doi:10.1002/acs.3044
19. Rahman Y, Xie A, Bernstein DS. Retrospective cost adaptive control: pole placement, frequency response, and connections with LQG control. *IEEE Contr Syst Mag*. 2017;37:85-121.
20. Islam SAU, Nguyen TW, Kolmanovsky IV, Bernstein DS. Data-driven retrospective cost adaptive control for flight control applications. *AIAA J Guid Contr Dyn*. 2021;44(10):1732-1758. doi:10.2514/1.G005778
21. Hoagg JB, Bernstein DS. Retrospective cost model reference adaptive control for nonminimum-phase discrete-time systems, part 1: the adaptive controller. Proceedings of the 2011 American Control Conference, 2933-2938. 2011. doi:10.1109/ACC.2011.5990986
22. Hoagg JB, Bernstein DS. Retrospective cost model reference adaptive control for nonminimum-phase discrete-time systems, part 2: stability analysis. *Proc Amer Contr Conf*. 2011;2927-2932. doi:10.1109/ACC.2011.5991465
23. Hoagg JB, Bernstein DS. Retrospective cost model reference adaptive control for nonminimum-phase systems. *AIAA J. Guid. Contr. Dyn.* 2012;35:1767-1786. doi:10.2514/1.57001
24. Mohseni N, Bernstein DS. Retrospective-cost-based model reference adaptive control of nonminimum-phase systems. *2023 American Control Conference (ACC)*. San Diego, CA; 2023:4247-4252. doi:10.23919/ACC55779.2023.10156011.

How to cite this article: Mohseni N, Bernstein DS. Retrospective-cost-based model reference adaptive control of nonminimum-phase systems. *Int J Adapt Control Signal Process*. 2024;38(7):2404-2422. doi: 10.1002/acs.3810